LOCAL ISOTROPY IN WIND TUNNEL TURBULENCE

by

V. A. SANDBORN AND R.D. MARSHALL

Prepared for
U. S. Army Research Grant
DA-AMC-28-043-64-G-9

FLUID MECHANICS PROGRAM
ENGINEERING RESEARCH CENTER
COLLEGE OF ENGINEERING
COLORADO STATE UNIVERSITY
FORT COLLINS, COLORADO

Technical Report

LOCAL ISOTROPY IN WIND TUNNEL TURBULENCE

by

V. A. SANDBORN AND R.D. MARSHALL

Prepared for
U. S. Army Research Grant
DA-AMC-28-043-64-G-9

FLUID DYNAMICS AND DIFFUSION LABORATORY
COLLEGE OF ENGINEERING
COLORADO STATE UNIVERSITY
FORT COLLINS, COLORADO

OCT 1965

LOCAL ISOTROPY IN WIND TUNNEL TURBULENCE

by

Virgil A. Sandborn and Richard D. Marshall

SUMMARY

Experimental evaluation of the longitudinal turbulent spectrum in the boundary layer of a long test section wind-tunnel are reported. The spectra agree very close with spectra reported for water flow in an ocean tidal channel and also for air flow over the sea surface. The spectra all agree with the predictions of local isotropy. The data reported were taken in a flat plate boundary layer at a station 69 feet from the tunnel entrance. The free-stream velocity was 30 feet per second. These flat plate boundary layer spectra differ greatly from previous data reported for flows with much small length dimensions.

INTRODUCTION

Mathematical treatment of turbulent boundary layers has been limited because an adequate model for the turbulent motion is lacking, (to close the formally indeterminate boundary layer equations for turbulent flow). The major treatment of the turbulent motion has been confined to the simplest case of non-shear flow having spherical symmetry: (isotropic turbulence) In the boundary layer, the overall turbulent motion is highly non-isotropic. However, Kolmogroff, ref. 1, has postulated that turbulent shear flows, such as boundary layers, may be "locally isotropic under certain conditions." Local isotropy assumes that at the higher wave numbers, or frequencies, when the turbulence loses its identity with its origin, the turbulent motion may be symmetrical.

The assumption of local isotropy requires that the Reynolds number of the flow be large. These conditions of large Reynolds number are only vaguely defined. Attempts to check the validity of the concept of local isotropy in boundary layers typical of those encountered on aircraft surfaces give negative results, ref. 2. Although some necessary conditions for local isotropy were found in a boundary layer with a "small" Reynolds number, the data also showed significant deviations from predictions of the theory.

In recent years measurements in flows having very large scales, such as ocean tidal channels, ref. 3, and atmospheric flows over the sea surface, ref. 4, displayed very strong evidence of local isotropy. Similar results have also been reported in the far regions of a jet, ref. 5. The concept of local isotropy can be of great value in atmospheric type of flows, ref. 6.

The present report demonstrates that it is possible to obtain turbulent boundary layers in a wind-tunnel which have sufficiently large scale to reach locally isotropic conditions.

TEST FACILITY

The wind tunnel employed in these measurements was specifically designed to obtain flows simulating those found in micrometeorology, ref. 7. Figure 1 shows a schematic diagram of the tunnel. The tunnel has a cross section of approximately 6 feet by 6 feet. The ceiling of the tunnel is adjustable for control of the axial pressure distribution. For the measurements reported herein, the ceiling was adjusted to give an approximately zero-pressure-gradient along the flow. The measurements of turbulence were made in the boundary layer developed along the floor of the wind tunnel. A free stream velocity of 30 feet per second was employed for all measurements reported in the present paper. The air temperature was approximately 70^{0}F and the air density was 1.9×10^{-3} slugs/ft^{3}.

Coarse gravel was attached to the floor and ceiling at the inlet contraction of the wind tunnel test section. This roughness was found to thicken the floor and ceiling boundary layers and to reduce the side wall effects. Measurements over the central two feet of the floor at a station 70 feet from the tunnel entrance showed that the boundary layer was reasonably uniform.

INSTRUMENTATION

Mean velocity profiles were taken with a pitot-static probe having a outside diameter of 1/4 inch. The probe was mounted on an actuator shown in Fig. 2. The pressure difference of the probe was fed into a capacitance type pressure transducer. The output voltage of the pressure transducer was fed into the y-axis of a x-y plotter. The x-axis of the plotter was driven by the actuator system, and is proportional to the distance above the wind tunnel floor. Figure 3 shows a typical plot of the dynamic pressure versus distance above the wind tunnel floor obtained directly from the x-y plotter. The plot qualitatively demonstrates the distribution of turbulence, as well as the mean velocity, in the boundary layer.

The longitudinal turbulent velocity fluctuations were measured with a constant-temperature hot-wire anemometer which was developed by Kovasynay, ref. 8 . This anemometer is fully transistorized and has a frequency response of approximately 5000 cycles per second. Figure 4 is a picture of the hot-wire probe and anemometer used in the experiment. The hot-wire probe has a replaceable tip alined to sense the u-component of turbulence. The sensing hot-wire element employed in the present measurements was a silver plated, 0.0002 inch diameter tungsten wire.

The output of the hot-wire anemometer was read on a true RMS electronic voltmeter which had a frequency response flat from 2 to 200,000 cycles per second. The output of the anemometer was recorded on FM magnetic tape at selected points in the boundary layer. The spectra of the turbulence signals were determined from the magnetic tape. An audio-wave-analyzer with an effective band width of 1.12 cycles per second was used to measure the energy density spectrum in the range from 1 to 16 cycles per second. From 16 to 2500 cycles per second a set of passive filters were used to measure the spectral energy density. These passive filters were the octave type varying in band width approximately proportional to the center frequency. The two sets of spectra measurements were matched at the 16 cycle per second point. The composite spectra F'(n) versus frequency f were normalized so that the integral under the curve would equal one; i.e.

$$\int_0^\infty F'(n)\, df = \frac{1}{G} \quad . \qquad (1)$$

Each value of energy density $F'(n)$ is multiplied by G in order to obtain the normalized value of $F(n)$.

Intermittency measurements were made with a percent time analyzer circuit developed by the CSU Fluid Dynamics and Diffusion Laboratory, ref. 9. This instrument and the analog instrument for measuring the spectra are a part of the CSU analog computer system shown in Fig. 5.

RESULTS AND DISCUSSION

A general evaluation of the conditions of local isotropy require the evaluation of, not only the longitudinal turbulent velocity component, but also, the transverse turbulent velocity components, ref. 2. The present check of local isotropy and those reported in references 3, 4 and 5 are based on the shape of the longitudinal turbulent velocity spectrum. The one dimensional spectral density shape may be regarded as a necessary condition for the existence of local isotropy, but not necessarily a sufficient condition. Further tests of the conditions of local isotropy should include measurements of the transverse turbulent velocity distribution.

Figure 6 shows the measured spectra at three distances above the wind tunnel floor. These data were taken at a station 69 feet from the entrance of the wind tunnel. The spectra are plotted in wave number coordinates, which are related to the frequency by the relations, ref. 10.

$$k = \frac{2\pi f}{U} \quad \text{and} \quad f(k) = \frac{U}{2\pi} \; F(n) \tag{2}$$

The data are also tabulated in Table I.

Kolmogoroff's hypothesis predicts the existence of an inertial sub-range in the spectral distribution. The spectral distribution for the inertial subrange has the form, ref, 3 and 4,

$$\overline{u^2} \; f(k) = \epsilon^{1/4} \, \nu^{5/4} \; F(k/k_s) \tag{3}$$

where ν is the kinematic viscosity, and $k_s = (\epsilon \nu^{-3})^{1/4}$. The total dissipation of turbulent energy per unit mass is represented by ϵ.

The total dissipation was not measured for the present flow. However, if the turbulence is locally isotropic, then the isotropic relations for ϵ may represent a good first approximation.

$$\epsilon = 15 \, \overline{u^2} \int_0^{\infty} k^2 \, f(k) dk \tag{4}$$

Figure 7 shows the values of ϵ calculated from equation (4) for the three spectra of Fig. 6. Figure 8 is a plot of the values of $\overline{u^2}$ f(k) versus $\epsilon^{1/4} \nu^{5/4}$ $F(k/k_s)$ for the three spectra. A definite region is found in which the spectra is a universal function of $F(k/k_s)$. The theory of local isotropy also predicts that the spectra in the universal region will vary as $k^{-5/3}$. The straight line drawn in Fig. 8 has a slope of -5/3. Thus, the measured spectra of turbulence agree well with the predictions of local isotropy.

The check of the turbulent spectra in the wind tunnel with those found in the atmosphere is a first step in establishing the use of the tunnel for detailed atmospheric modeling. Figure 9 compares the spectra measured at $y/\delta = 0.500$ with a spectra measured in an ocean tidal channel and a spectra measured in the atmospheric flow over the sea surface. These three widely different spectra show very good agreement when plotted in the form predicted by local isotropy. In each of the spectra plotted in Fig. 9 the values of ϵ was obtained from equation (4). Figure 9 appears to be very strong evidence that local isotropy exists in the three widely different turbulent flows. The agreement of the three spectra in the region beyond the inertial subrange, where $f(k) \propto k^{-5/3}$, should also be noted.

At the small wave numbers the three spectra vary widely. The wind tunnel spectra shows more evidence of its origin than does the other two spectra. No doubt the small wave number region is a function of the Reynolds number associated with the flow. Exactly what Reynolds number determines the degree of local isotropy is not firmly established. Gibson, ref. 5 following the lead of Corrsin, ref. 11, suggests that $R_\lambda = \frac{\sqrt{\overline{u^2}}\lambda}{\nu}$ is the determining factor, where $\sqrt{\overline{u^2}}$ is the rms longitudinal turbulent velocity and $\lambda = \frac{U}{2\pi}\left(\int_0^\infty f^2 F(n)\,df\right)^{-1/2}$ is the microscale of the turbulence. A value of R_λ greater than 700 was suggested as necessary to produce local isotropy. The present data have values of R_λ no greater than 400. Previous turbulent boundary layer measurements in wind tunnels have reach values of R_λ greater than 800 without indicating evidence of local isotropy, ref. 2 and 10. Figure 10 compares the present measured spectra with other reported wind tunnel boundary layer spectra, ref. 10 and 12. The spectra reported by Gibson is also shown in Fig. 10. Evidently, the determining Reynolds number, if one exists for local isotropy, is not that given by R_λ .

One obvious reason that local isotropy is not observed in the "small" scale boundary layers of Fig. 10 has been traced to "local" intermittency, ref. 13. In the turbulent flows of ref. 2 and 10, the high frequency or large wave number region of the turbulence was not continuous in time. In other words, the high frequency turbulence was found to be intermittent or to appear in bursts. This high frequency intermittency proved to be roughly independent of location in the boundary layer and to be a function of wave number only. The intermittency of the high frequency components of the present turbulent signals are shown in Fig. 11. In the present experiments, high frequency intermittency was encountered only at frequencies in excess of those important in the inertia subrange.

The mean velocity distribution for the 69 foot station is shown in Fig. 12. The longitudinal turbulent velocity distribution at the 69 foot station is shown in Fig. 13. Figure 14 and 15 show the development of the boundary layer down the wind tunnel. Although this set of boundary layer profiles were taken under approximately the same conditions as the data presented for the 69 foot station, the actual measurements were made several months earlier.

CONCLUDING REMARKS

The measurements reported herein demonstrate that the boundary layer flow in a long wind tunnel has turbulence conditions similar to that found in atmospheric flows. These wind-tunnel flows appear to contain large regions within the inertial subrange which implies local isotropy. The existence of local isotropy will greatly simplify the evaluation of such turbulent quantities as the total dissipation of turbulent energy. The existence of local iostropy in a controlled flow field, such as a wind tunnel, will also make experimental study of this type of flow easier. It should be possible to determine the parameters governing the onset of local isotropy, and secondly to determine the extent that isotropic relations can be used if local isotropy exists.

REFERENCES

1. Kolmogoroff, A.: The Local Structure of Turbulence in Incompressible Viscous Fluid for Very Large Reynolds Numbers. Comp. Rend., Acad. Sci. URSS, Vol. XXX, No. 4, 1941.

2. Sandborn, V. A., and Braun, W. H.: Turbulent Shear Spectra and Local Isotropy in the Low-Speed Boundary Layer, NACA TN 3761, 1956.

3. Grant, H. L, Stewart, R. W. and Moilliet, A.: Turbulence Spectra from a Tidal Channel. Jour. of Fluid Mech., Vol. 12, 1962.

4. Pond, S., Stewart, R. W. and Burling, R. W.: Turbulence Spectra in Wind Over Waves. Jour. of the Atmospheric Sci., Vol. 20, 1963.

5. Gibson, M. M.: Spectra of Turbulence in a Round Jet. Jour. of Fluid Mech., Vol. 15, part 2, 1963.

6. Batchelor, G. K.: Theory of Homogeneous Turbulence. Cambridge University Press, 1953.

7. Plate, E. J., and Cermak, J. E.: Micrometeorological Wind Tunnel Facility. Final Report, Contract No. DA-36-039-SC-80371. For U. S. Army, Fluid Dynamics and Diffusion Lab., CSU, Fort Collins, Colorado.

8. Kovasznay, L. S. G., Miller, L. T. and Vasudenva, B. R.: A Simple Hot-Wire Anemometer; Project Squid Technical Report JHU-22-p. (John Hopkins University), 1963.

9. Finn, C. L., and Sandborn, V. A.: Instrument for Measuring the Intermittency of Quasi-Steady Signals. Fluid Mechanics Paper No. 3, Colorado State University, Fort Collins, Colorado.

10. Sandborn, V. A. and Slogar, R. J.: Longitudinal Turbulent Spectrum Survey of Boundary Layers in Adverse Pressure Gradients. NACA TN 3453, 1955.

11. Corrsin, S.: NACA. Research Memorandum, R. M. 58B11, 1958.

12. Klebanoff, P. S.: Characteristics of Turbulence in a Boundary Layer with Zero Pressure Gradients. NACA TN 3178, 1954.

13. Sandborn, V. A.: Measurements of Intermittency of Turbulent Motion in a Boundary Layer. Jour. Fluid Mechanics, Vol. 6, part 2, 1959.

TABLE I - TURBULENT SPECTRA

Distance Above The Floor, Inches	4"	12"	18"
Mean Velocity, U ft/sec	22.8	27.4	29.4
Longitudinal Turbulent Velocity, $\sqrt{u^2}$, ft/sec	2.00	1.43	.782
Total Dissipation Of Turbulent Energy, ϵ, ft^2/sec^3	8.36	2.01	.508
Microscale, λ_x, ft.	.0374	.0546	.0594
k_s, ft^{-1}	1007	723	828

f	F(n)	f	F(n)	f	F(n)
1	6.06^{-2}	1	6.516^{-2}	1	5.599^{-2}
2	5.925	2	6.384	2	5.47
3	5.78	3	5.412	3	5.30
4	5.488	4	5.000	4	5.044
6	5.18	6	4.43	6	4.53
8	4.436	8	2.982	8	4.08
10	3.36	10	1.981	10	3.588
12	2.84	12	1.740	12	3.419
14	2.277	14	1.482	14	2.582
16	1.875	16	1.171	16	2.042
20	1.32	20	7.35^{-3}	20	1.399
25	7.385^{-3}	25	4.319	25	6.45^{-3}
32	4.656	32	3.03	32	4.29
40	3.28	40	1.82	40	3.181
50	2.654	50	1.568	50	2.327
64	1.632	64	1.03	64	1.776
80	1.172	80	6.798^{-4}	80	1.097
100	7.94^{-4}	100	3.972	100	7.22^{-4}
125	5.65	125	2.94	125	4.952
160	4.10	160	2.122	160	3.352
200	2.46	200	1.494	200	1.819
250	1.278	250	7.30^{-5}	250	9.40^{-5}
320	9.03^{-5}	320	5.19	320	7.11
400	5.355	400	2.892	400	3.677
500	3.461	500	1.824	500	2.242
640	1.682	640	8.95^{-6}	640	9.50
800	9.251^{-6}	800	4.59	800	5.43
1k	3.692	1k	2.21	1k	2.159
1.25k	1.703	1.25k	8.671^{-7}	1.25k	1.121
1.6k	5.84^{-7}	1.6k	2.661	1.6k	3.268^{-7}
2.0k	2.041	2.0k	1.016	2.0k	2.326
2.5k	5.782^{-8}	2.5k	3.628^{-8}	2.5k	2.758

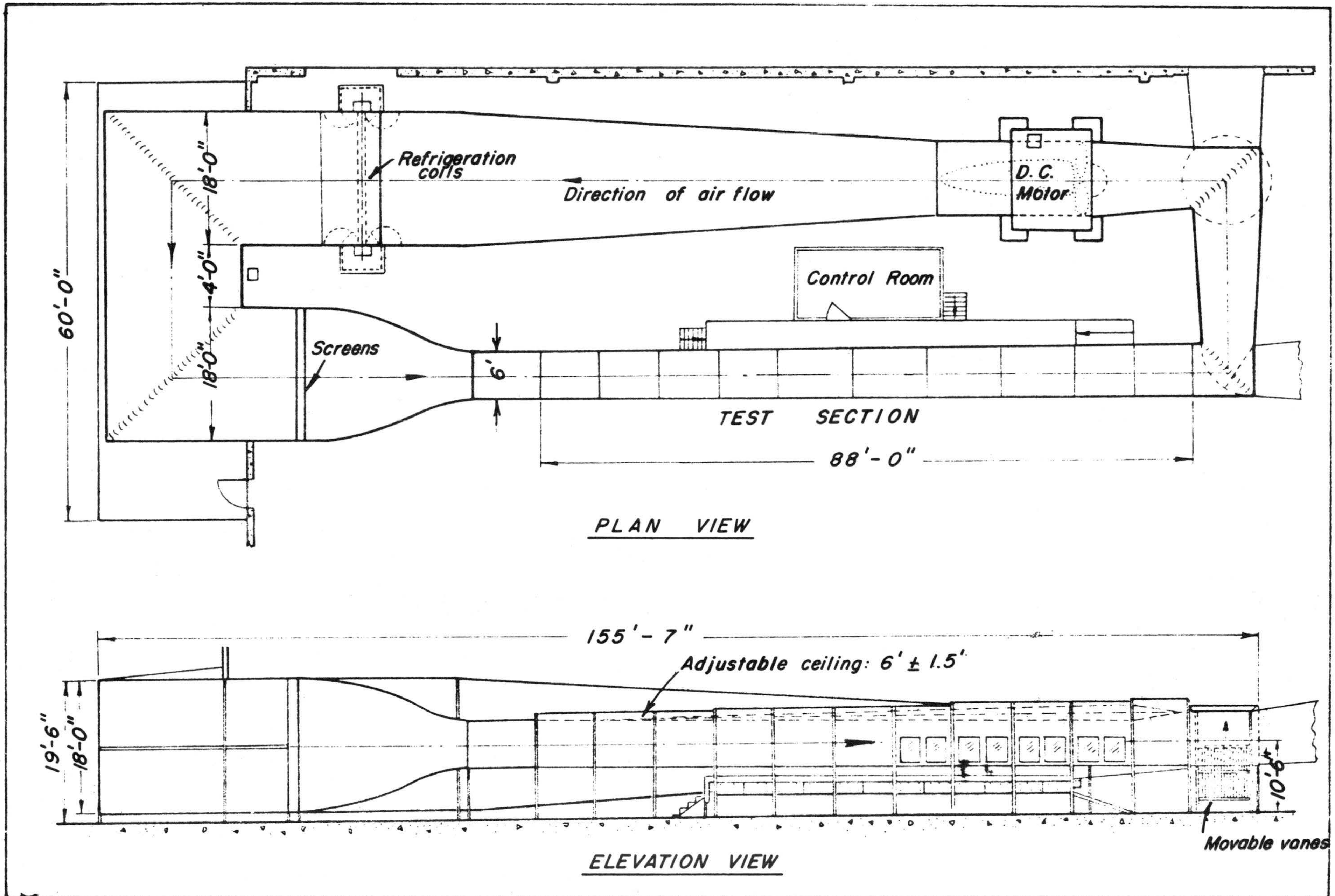

FIG. I LARGE WIND TUNNEL

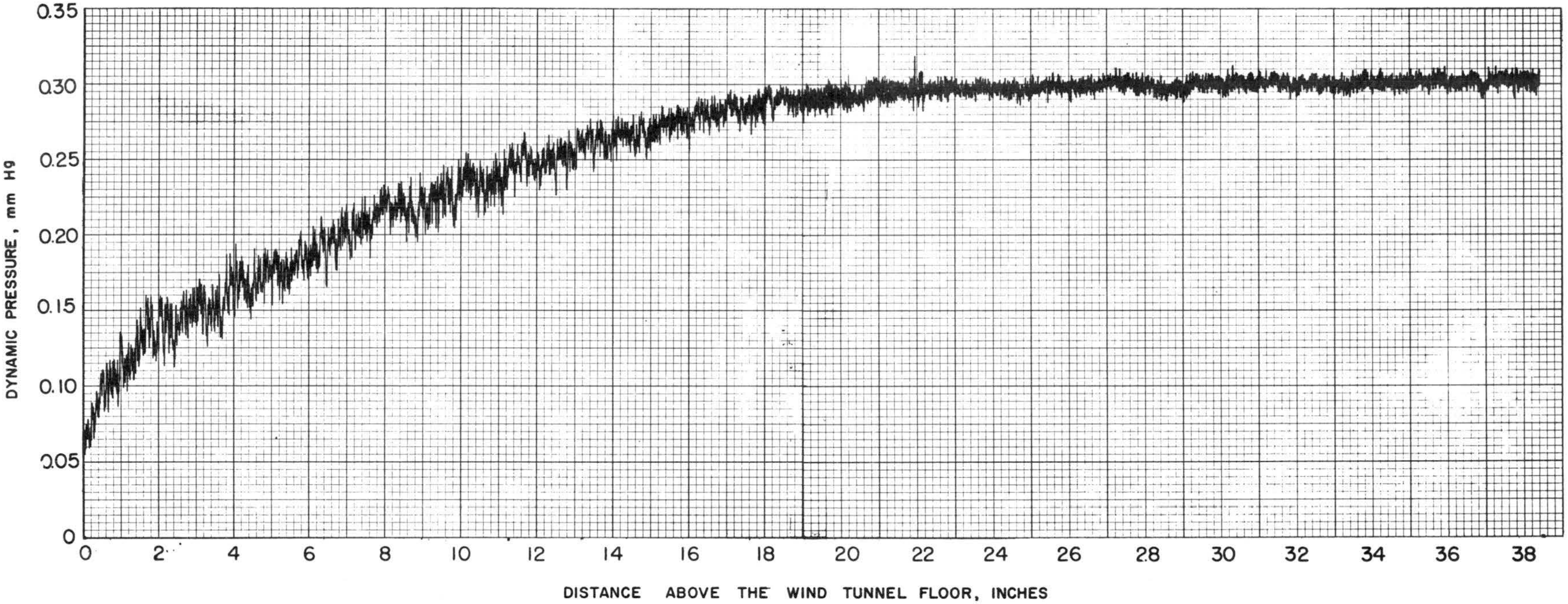

FIGURE 3 TYPICAL DYNAMIC PRESSURE MEASUREMENTS IN THE BOUNDARY LAYER. STATION 69 FEET FROM ENTRANCE

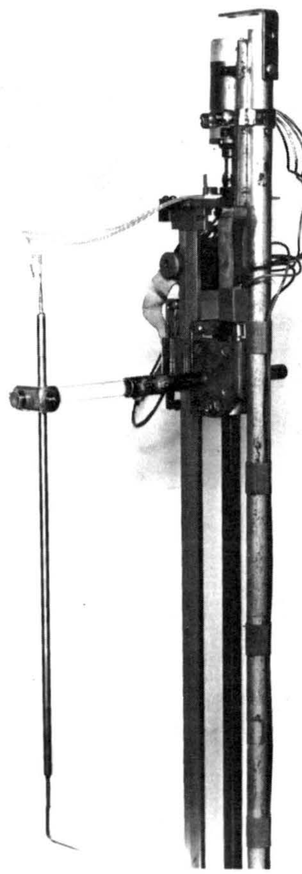

Figure 2. Probe and Actuator.

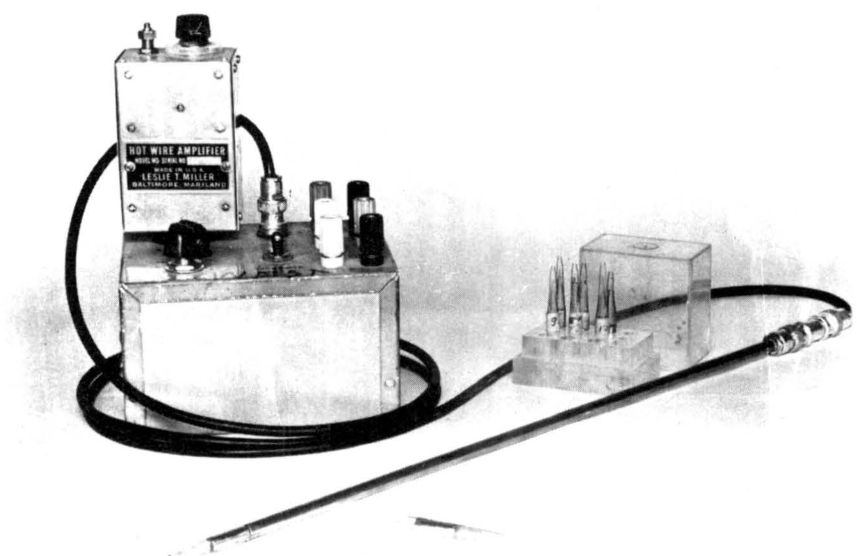

Figure 4. Hot-Wire Anemometer and Probes.

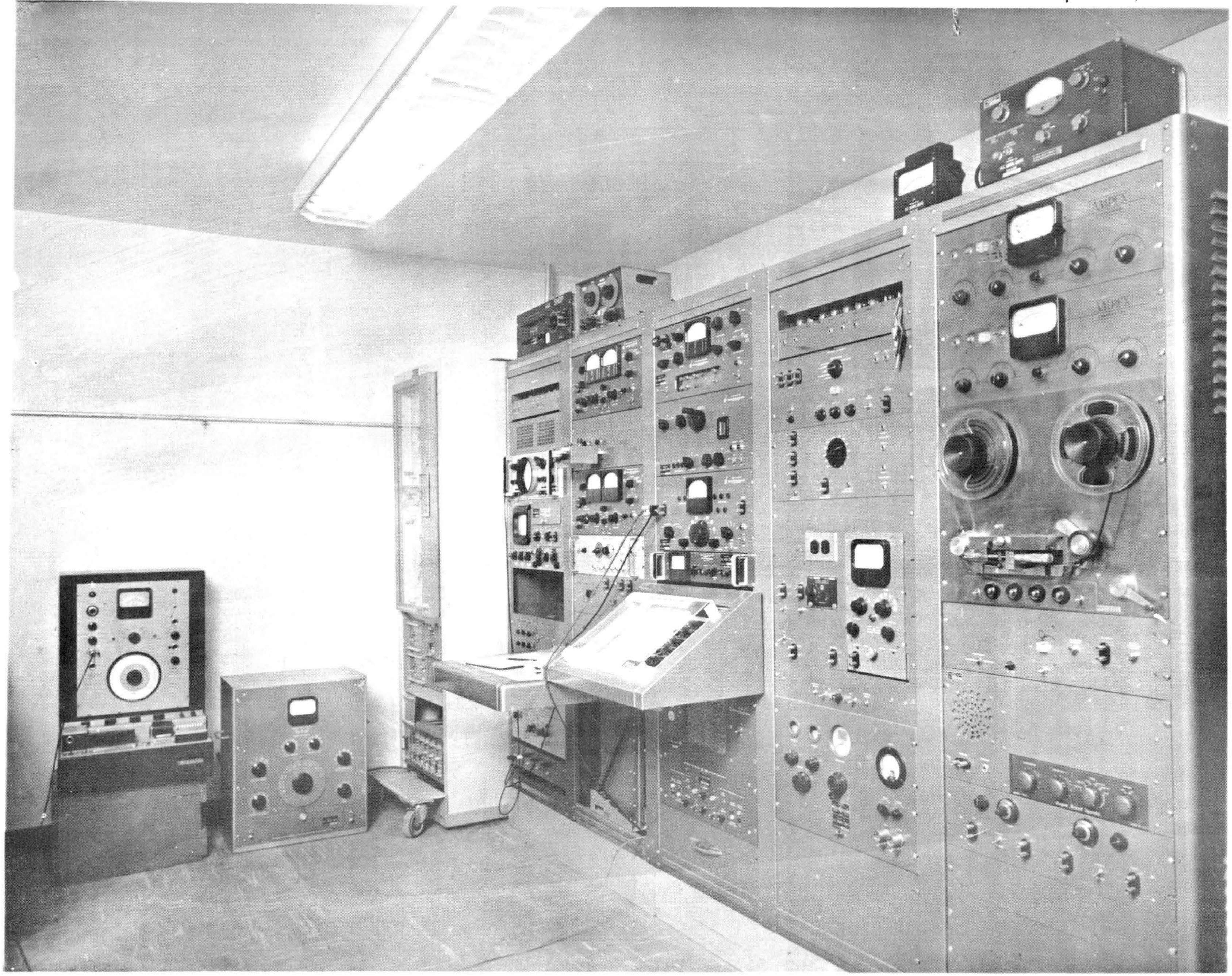

Figure 5. Analog computer.

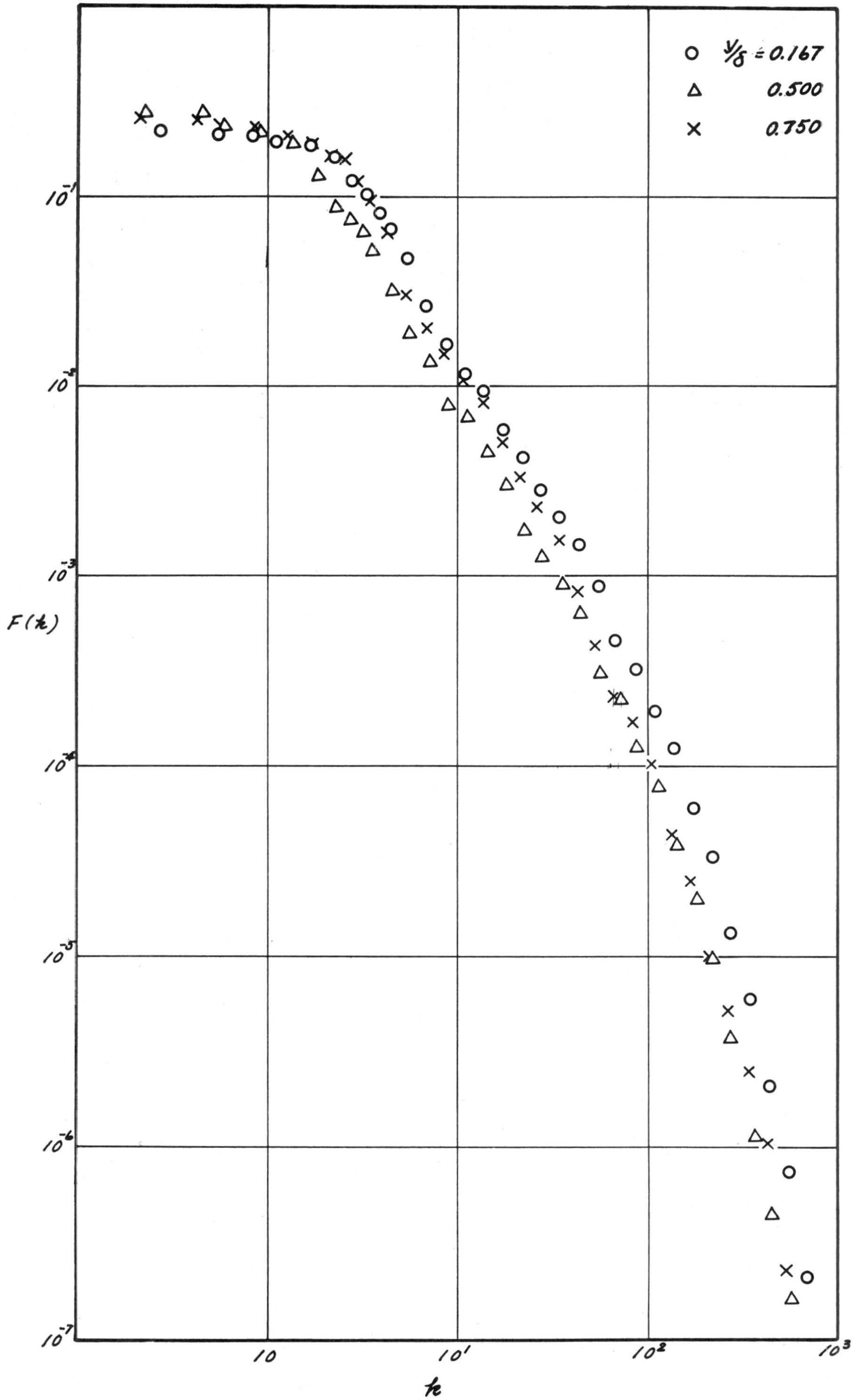

Figure 6. Spectral energy distribution

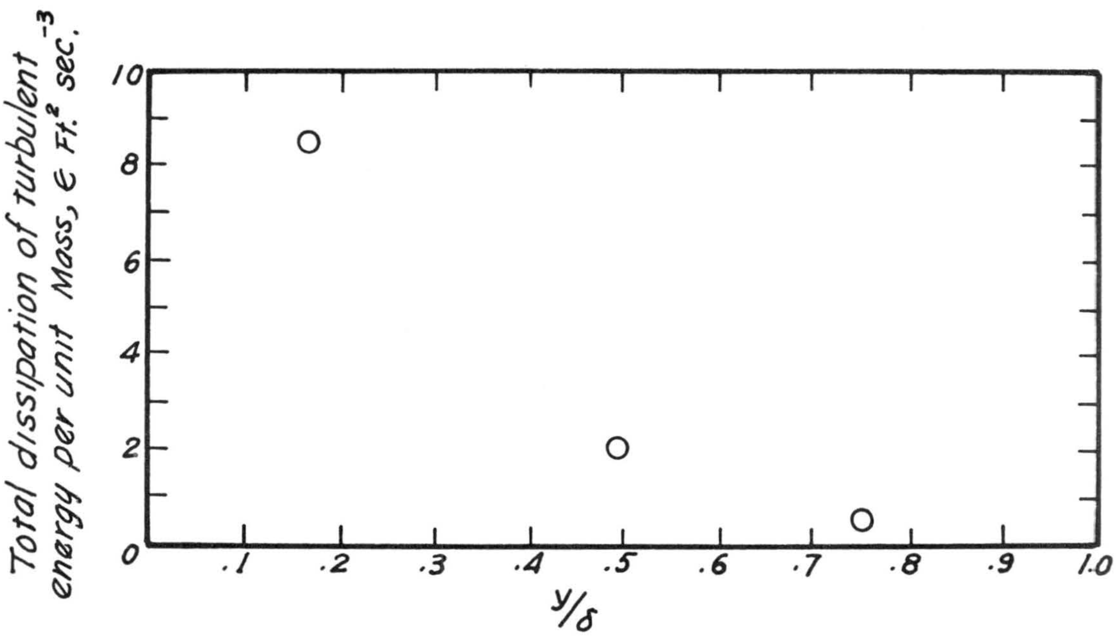

Figure 7 Variation of the dissipation of turbulent energy with distance from the wind tunnel floor.

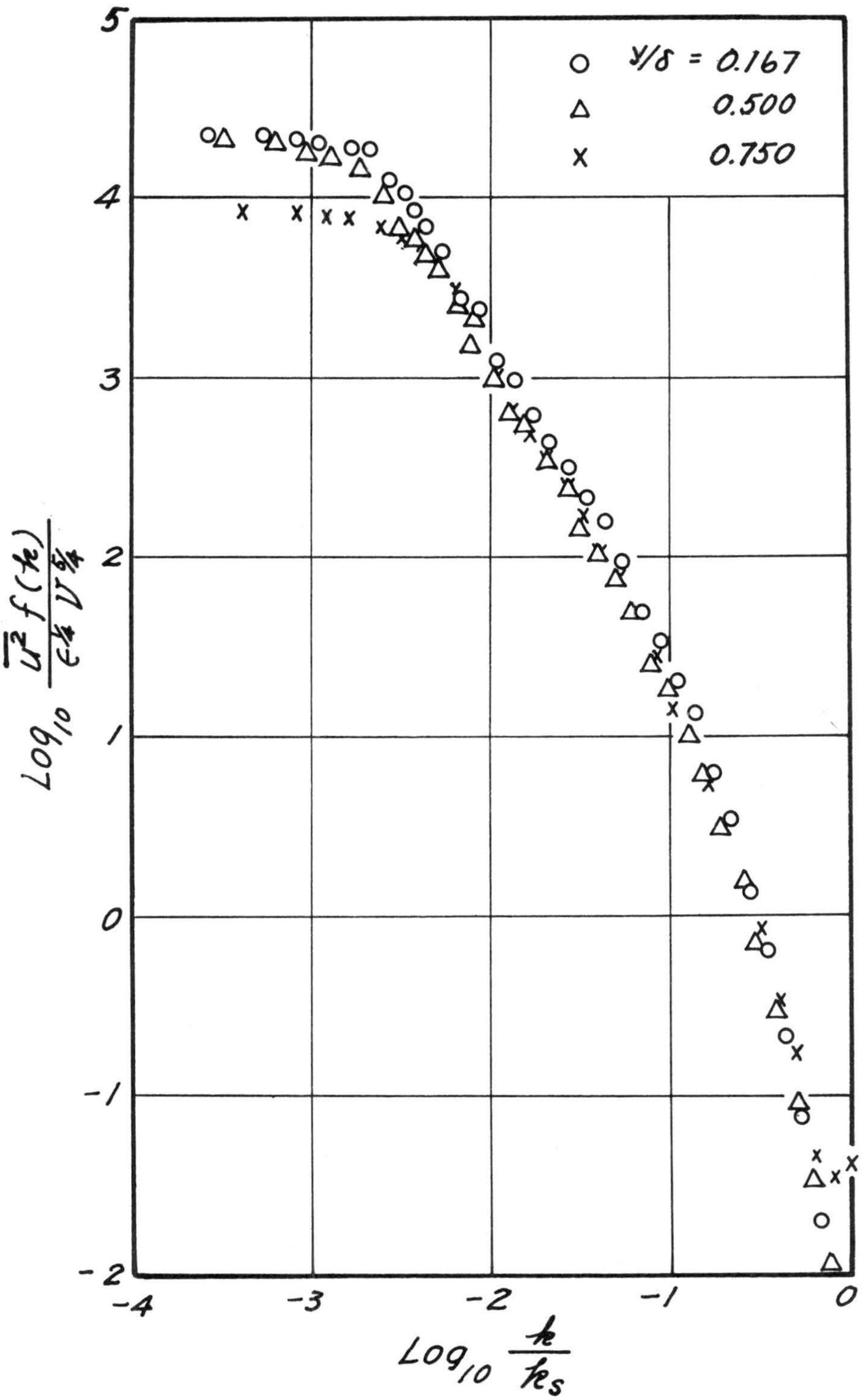

Figure 8. Normalized energy spectra

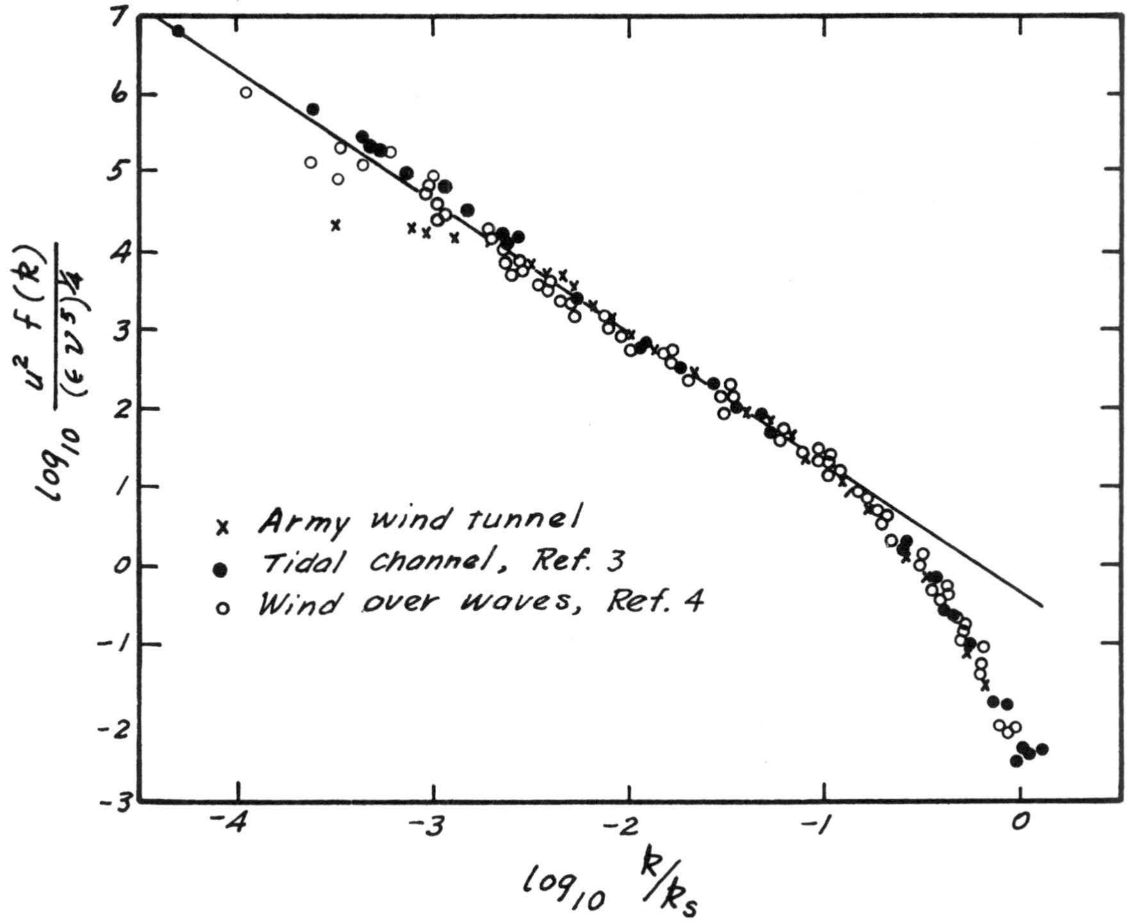

Fig. 9. Comparison of spectra measurements from the army wind tunnel, an ocean tidal channel and air flow over the sea surface

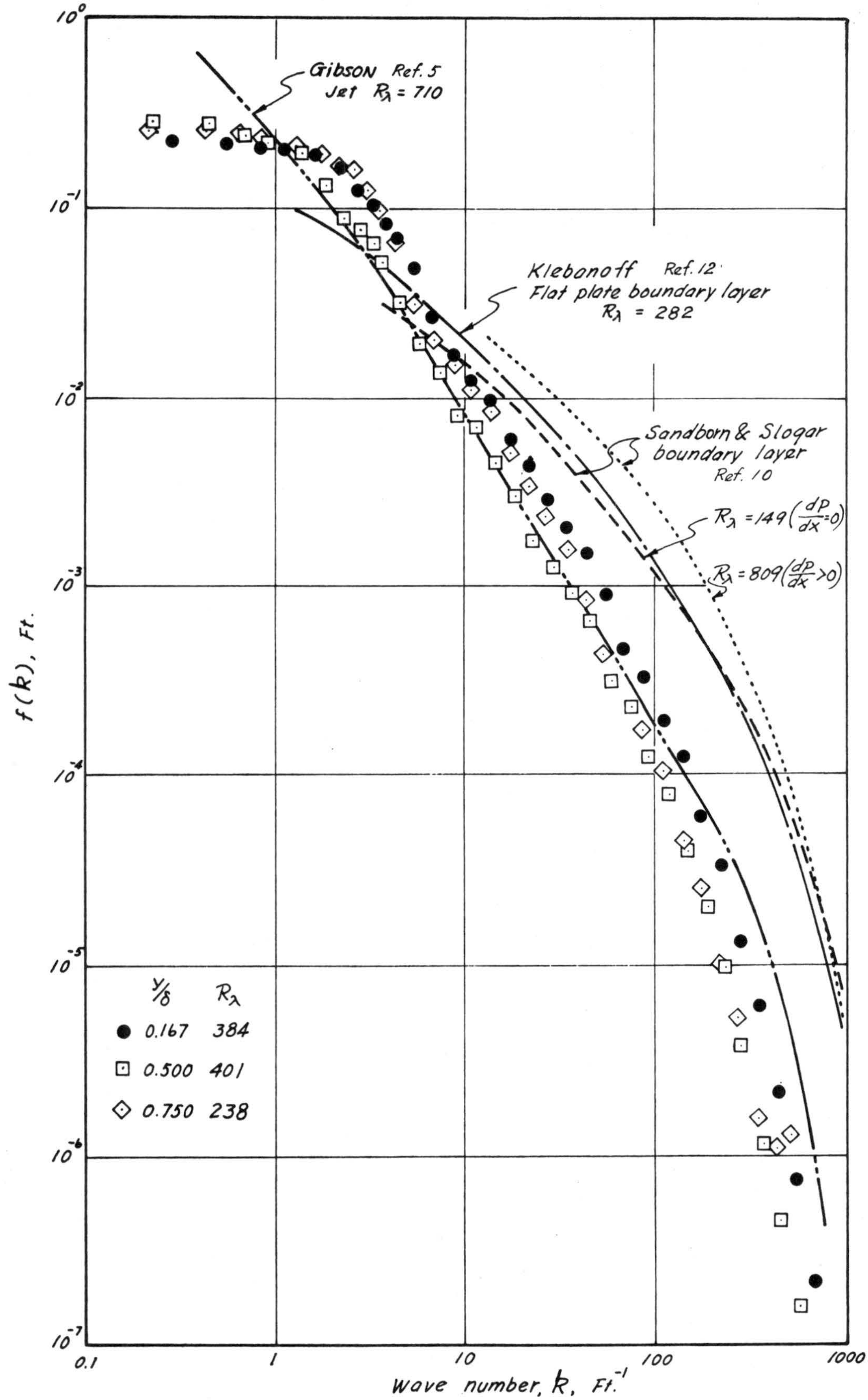

Fig. 10 Spectral energy density measured in the army wind tunnel compared with aircraft type boundary layer spectral

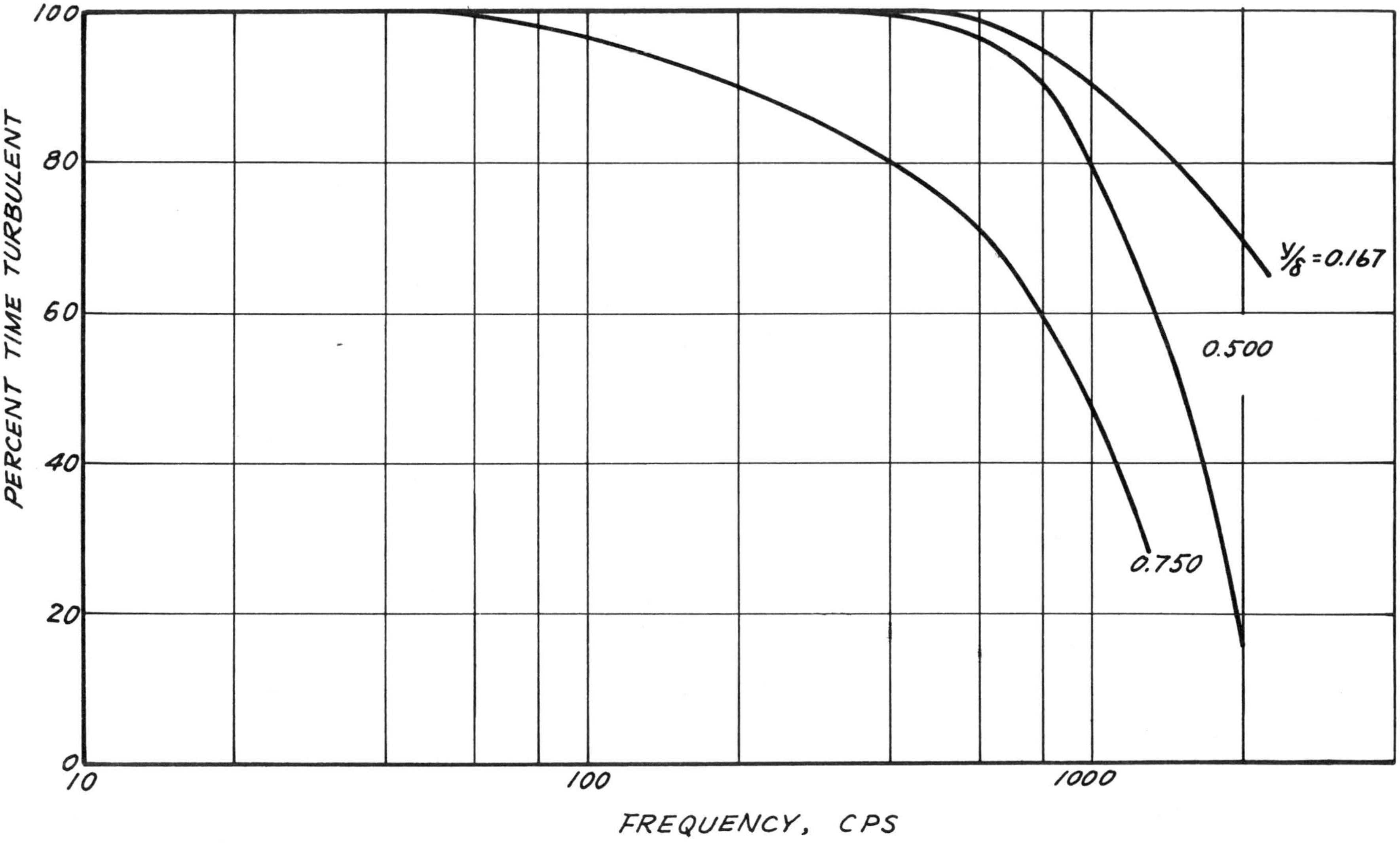

Figure 11 Measured intermittency at the high frequencies

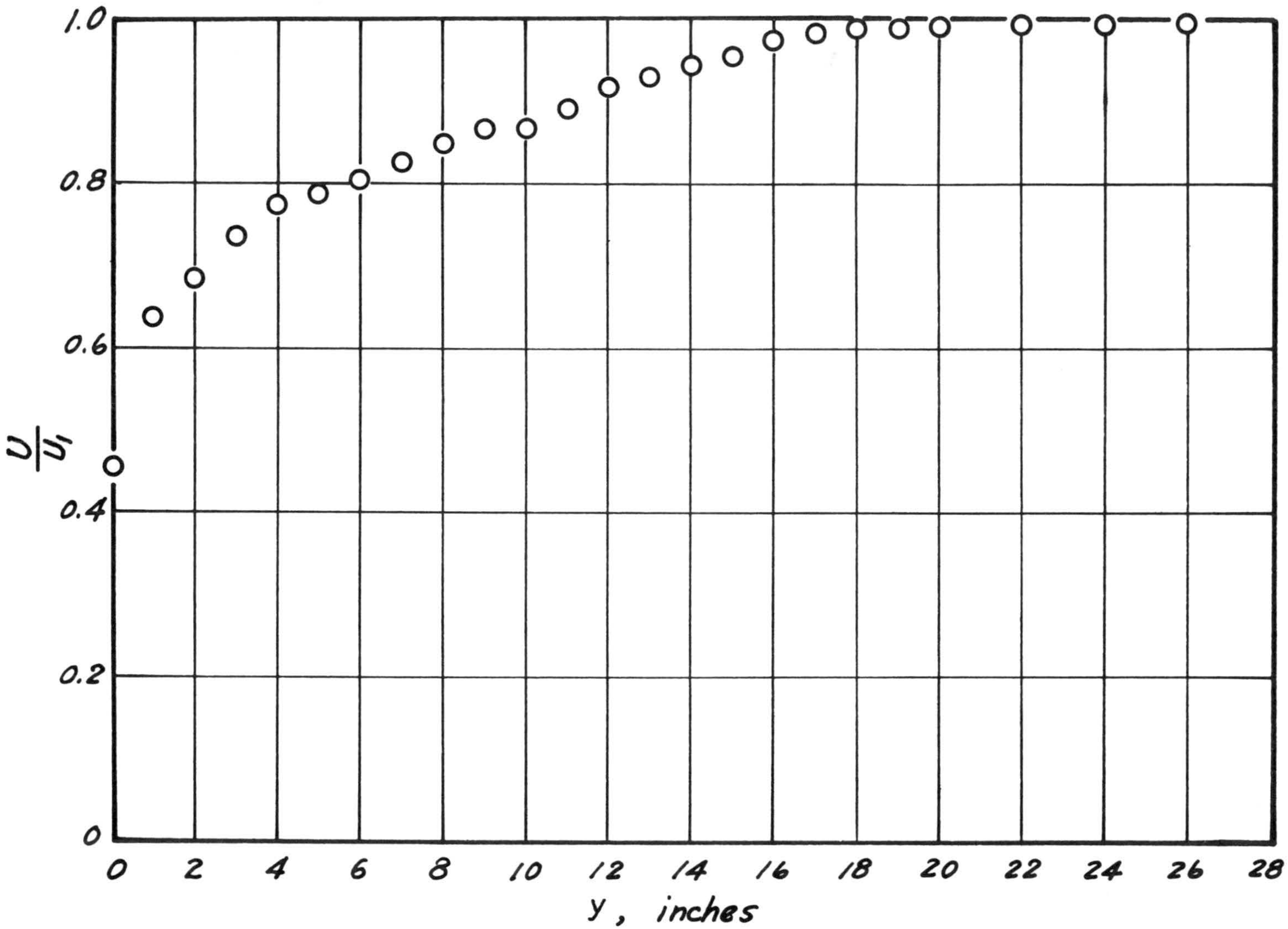

Figure 12. Mean velocity distribution at 69 feet; $T_a = 72°F$, $V_1 = 30$ fps $P_{at} = 25.15''$ Hg.

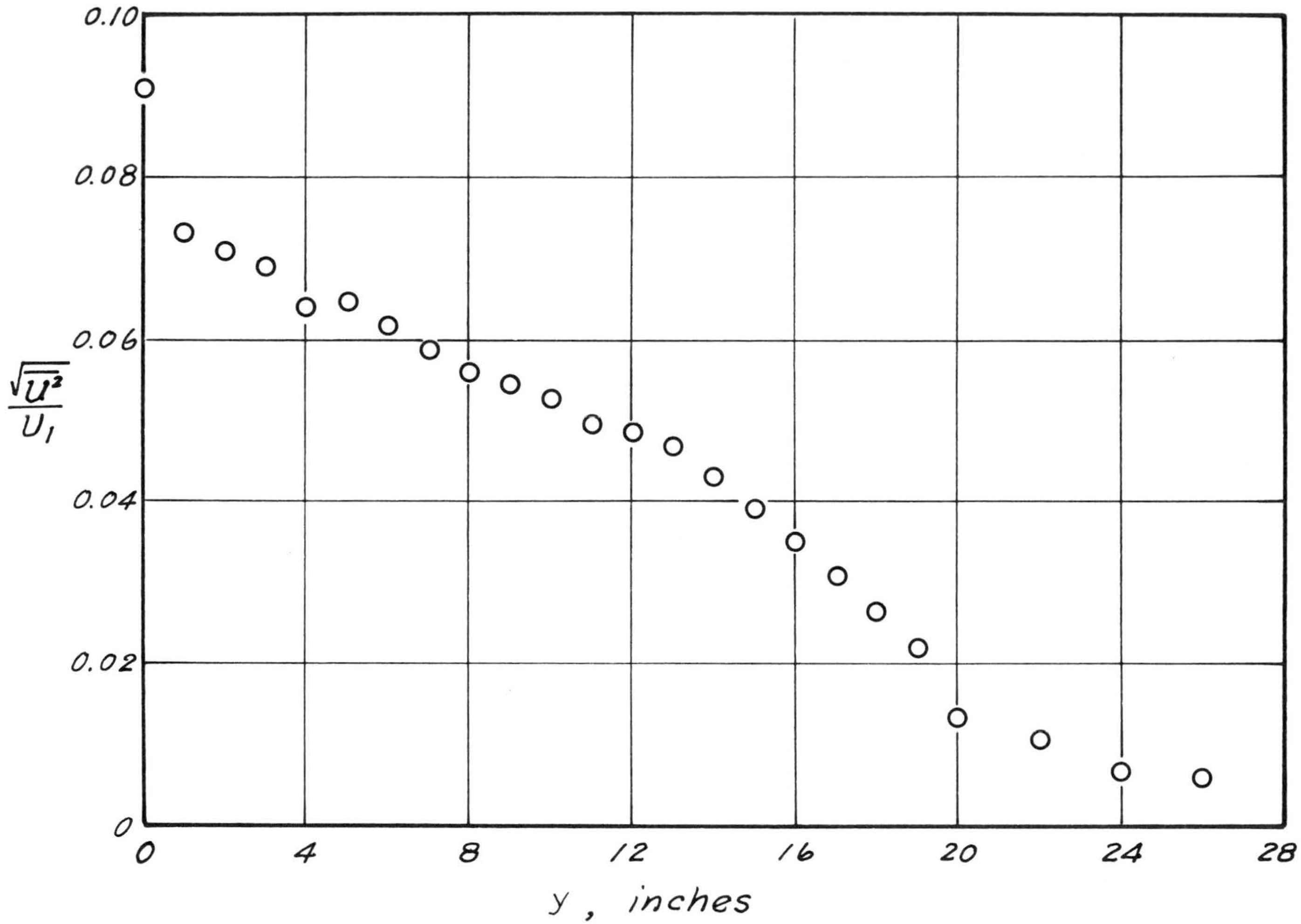

Figure 13. Longitudinal turbulent velocity distribution 69 feet.
$V = 30$ fps $T_a = 72°F$ $P_{at} = 25.15''$ Hg

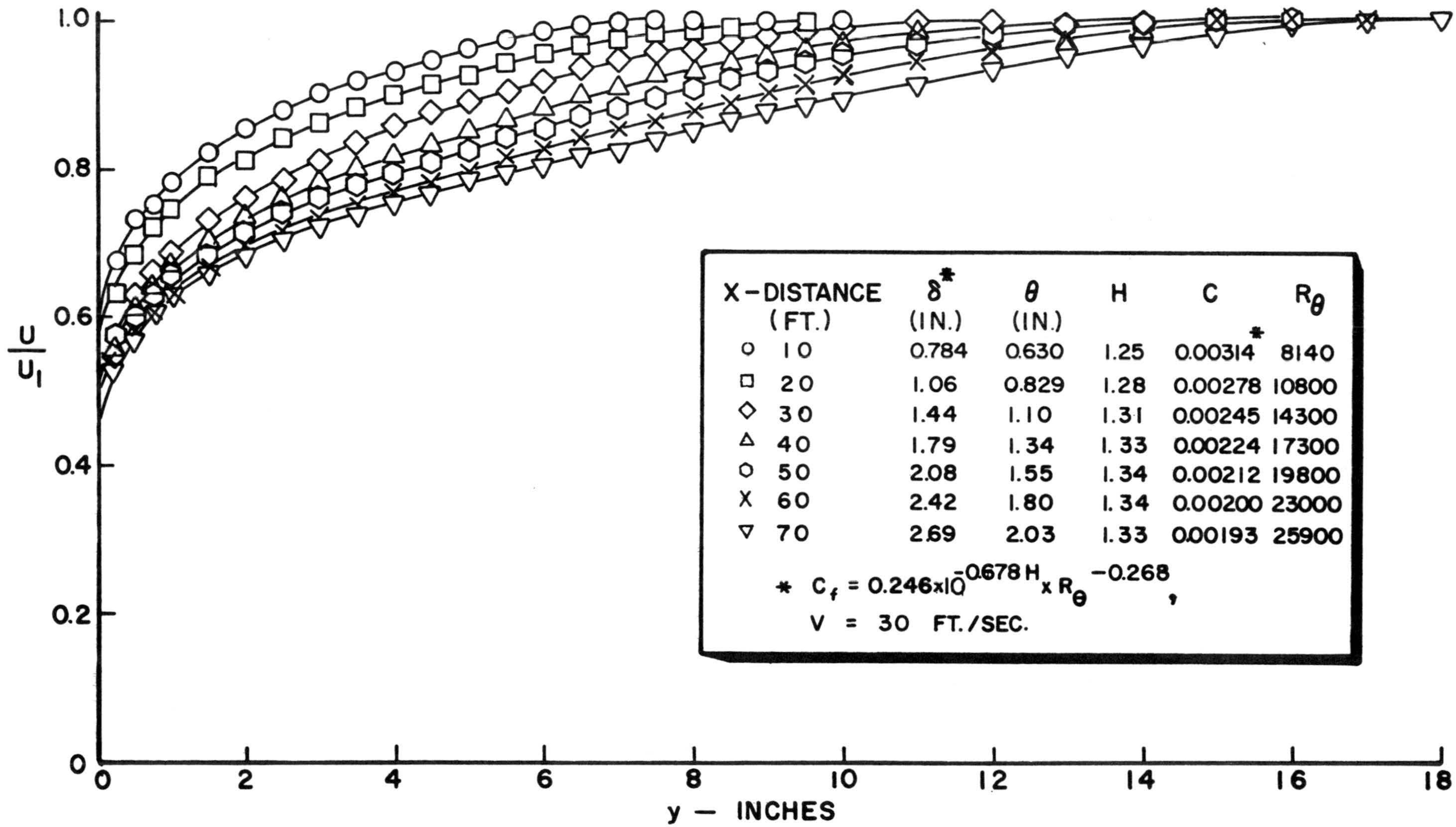

FIGURE 14 MEAN VELOCITY DISTRIBUTIONS ALONG THE WIND TUNNEL FLOOR

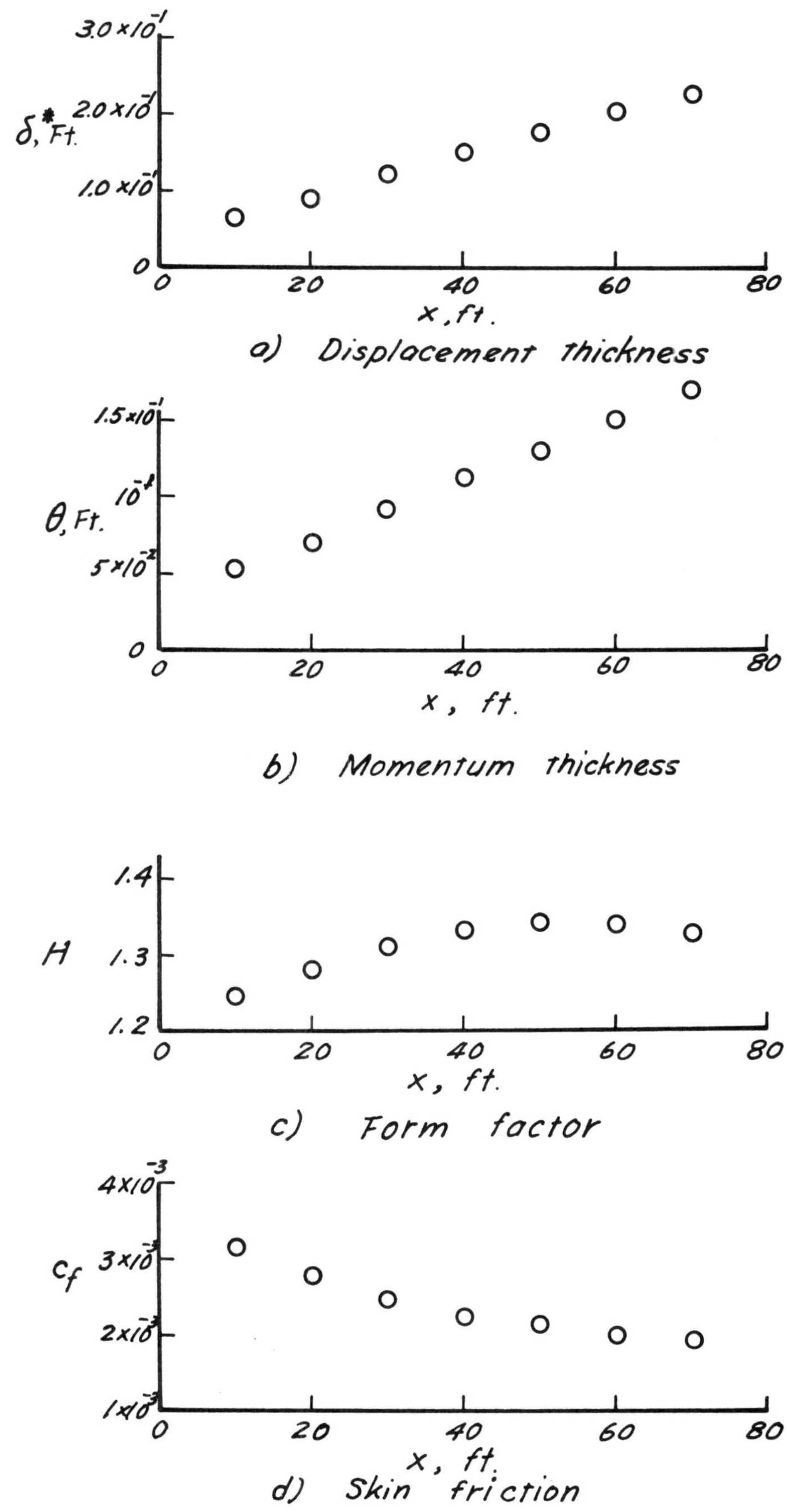

Figure 15 Boundary layer development along the wind tunnel floor